Enhancement of resistance anomalies by diffuse boundary scattering in multiprobe ballistic conductors

R. J. Blaikie
Microelectronics Research Centre, Cavendish Laboratory, University of Cambridge, Cambridge CB3 OHE, United Kingdom

K. Nakazato
Hitachi Cambridge Laboratory, Madingley Road, Cambridge CB3 OHE, United Kingdom

J. R. A. Cleaver and H. Ahmed
Microelectronics Research Centre, Cavendish Laboratory, University of Cambridge, Cambridge CB3 OHE, United Kingdom

(Received 6 July 1992)

We have extended the billiard-ball model for multiprobe ballistic conductors to include explicitly diffuse boundary scattering. We find that the negative zero-field bend resistance and the quenching of the Hall effect are both enhanced by diffuse boundary scattering, due to the effects of nonzero length leads on the angular distribution of the electrons entering the junction. Two peaks are predicted in the longitudinal magnetoresistance and verified by measurements on a multiprobe wire fabricated in $GaAs/Al_xGa_{1-x}As$ heterostructure using p-type implants to provide the lateral confinement.

The effects of reducing some or all of the dimensions of a multiprobe conductor to less than the electron mean free path have been widely studied both experimentally and theoretically.[1] In this ballistic transport regime, boundary scattering effects can dominate the device resistance, so that the geometry of the junction regions and the nature of the scattering of electrons from the device boundaries become very important. Anomalous effects are observed when the Hall resistance R_H and the bend resistance R_B are measured at a junction between narrow wires in a two-dimensional electron gas.[2-5] Around zero magnetic field, the Hall resistance is "quenched" (less than the value for a bulk sample) or even becomes negative and then rises steeply to a "last plateau" at a field below the threshold for quantum Hall plateaus. The bend resistance is negative at zero magnetic field and then "overshoots" to a positive value before dropping to zero at higher fields. These phenomena result from the ballistic nature of the electron transport across the junction, and can be explained by a semiclassical billiard-ball model,[6] where the electrons behave like classical billiard balls and scatter completely specularly from the device boundaries. Upon comparison with experiment,[7] this simple model accurately predicts the magnitudes and the magnetic field positions of the "last plateau" in the Hall resistance and the positive overshoot in the bend resistance. However, the magnitude of the zero-field negative bend resistance predicted was found to be approximately half of the measured value.

We have extended the semiclassical billiard-ball model to include diffuse scattering at the sample boundaries, and we find that the negative zero-field bend resistance and the quenching of the Hall resistance are both enhanced when the boundary scattering becomes diffusive. The current and voltage probe contacts form electron reservoirs, which are connected to the junctions by finite-length leads. These leads act as spatial filters when there is some diffuse boundary scattering, and so tend to collimate the electron distribution entering the junction. We find also that the anomalous resistance effects are still present in the case of completely diffuse boundary scattering, confirming that these effects are dominated by electrons passing straight through the junction.[8]

We consider a hard-walled system with two junctions (Fig. 1, inset), in which a channel of length l is connected at junctions having radii of curvature r to six probes by leads of length l'. The channel and leads are of width w.

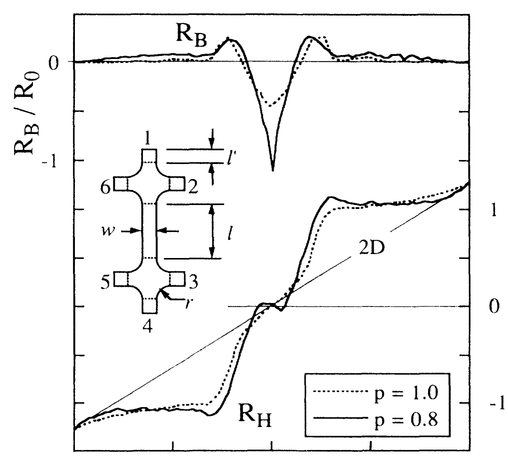

FIG. 1. Bend resistance R_B and Hall resistance R_H calculated for a six-probe geometry (inset). Dashed lines: purely specular boundary scattering, $p=1.0$. Solid lines: some diffuse boundary scattering, $p=0.8$. Device parameters used are $l/w=15$, $l'/w=7.5$, and $r/w=2$. The straight line is R_H for a macroscopic two-dimensional (2D) sample.

Following the work of Beenakker and van Houten,[6] we estimate the probability for an electron injected from probe i to be transmitted into probe j, T_{ji}, and to be reflected back into probe i, T_{ii}, by following a large number (typically $>10^4$) of classical electron trajectories through the device. We inject the electrons into the leads with a uniform distribution across the lead width, and angular distribution $P(\alpha)=(\frac{1}{2})\cos\alpha$, where α is the angle with the lead axis. Once the transmission and reflection probabilities are known, then the four-terminal device resistances $R_{ij,kl}\equiv(\mu_k-\mu_l)/eI_{i\to j}$ (source i, drain, j, voltage probes k and l) are obtained by solving the Büttiker equation,[9]

$$(h/2e)I_i=(N_i-T_{ii})\mu_i-\sum_{j\neq i}T_{ij}\mu_j \ , \tag{1}$$

which relates I_i, the current in lead i, to the chemical potentials μ_j of the reservoirs attached to the leads. The transmission and reflection probabilities are normalized such that

$$\sum_{j\neq i}T_{ji}+T_{ii}=N_i \ , \tag{2}$$

with N_i the number of propagating modes in lead i. We assume that all leads are identical, so that $N_i\equiv N$ for all i, and in the semiclassical limit we also assume that $N=k_F w/\pi$, where k_F is the Fermi wave vector. Diffuse boundary scattering is assumed to be elastic and is introduced into our model via the specularity coefficient p, such that at each boundary collision the electron will scatter diffusely with a probability $(1-p)$. If diffuse boundary scattering does occur at any particular boundary collision, then the electron is reemitted into the device at the collision point, with a random angle (uniformly distributed between $-\pi/2$ and $+\pi/2$) relative to the boundary normal.

In Fig. 1 we show the Hall resistance $R_H=R_{14,53}$ and bend resistance $R_B=R_{13,54}$ calculated using this model for a device having $l/w=15$, $l'/w=7.5$, and $r/w=2$. In the simulation results, resistances are normalized by the contact resistance of the leads $R_0\equiv(h/2e^2)\pi/k_F w$, and magnetic fields are normalized by $B_0\equiv mv_F/ew$, where v_F is the Fermi velocity. For the case of completely specular boundary scattering ($p=1$) there is a negative zero-field R_B with positive overshoot at $\beta\equiv B/B_0\approx0.5$, and a last plateau in R_H which starts at $\beta\approx0.5$. No quenching of the Hall effect is observed for $\beta<0.5$. The situation changes greatly with the introduction of some diffuse boundary scattering ($p=0.8$). This causes the negative zero-field R_B to be enhanced to a value more than twice that for the case of completely specular boundary scattering, as well as causing the weak field R_H to become negative at $\beta\approx0.1$, whereas it was not even quenched when the boundary scattering was purely specular. Other effects observed are a movement of the position of the positive overshoot in R_B to a lower field (with the magnitude of the overshoot remaining unchanged), as well as flattening and broadening of the last plateau in R_H. Although we have performed no comparative study, we believe that these dramatic enhancements of the resistance anomalies for only a mild amount of diffuse boundary scattering account for the discrepancy in the magnitude of the negative zero-field R_B between experimental results and the predictions of Beenakker and van Houten.[7]

We now go on to consider a mechanism for these enhancements by looking at a simplified, symmetrical four-terminal device structure with junction radii r and lead lengths l' (Fig. 2, inset). For this structure the Hall resistance and bend resistance are calculated from T_F, the transmission probability of electrons into the front probe, and T_L and T_R, the transmission probabilities into the left and right probes, respectively. The negative zero-field bend resistance is given by $R_B(0)/R_0=N(T_S-T_F)/[4T_S(T_S+T_F)]$, where we use $T_L=T_R=T_S$ at zero magnetic field. Figure 2 shows the variation of T_F, T_S, and $R_B(0)$ with specularity coefficient p for a junction with $r/w=2$ at three values of normalized lead length l'/w. We see that, for all values of l'/w, T_F and T_S both decrease monotonically as p is reduced, since diffuse boundary scattering will cause more electrons to be backscattered into the lead from which they originated. However, when the electrons are injected directly into the junction ($l'/w=0$) there is no variation of $R_B(0)$ with p, and it requires nonzero lead length for the enhancement to become effective. Thus the enhancement of $R_B(0)$ is essentially a property of the leads, and not of the junction itself. We note that even for completely diffuse boundary scattering ($p=0$) $R_B(0)$ is enhanced relative to the $p=1$ case, in contrast to other predictions[10] that assume that electrons randomly scattered (from both boundaries and impurities) will have

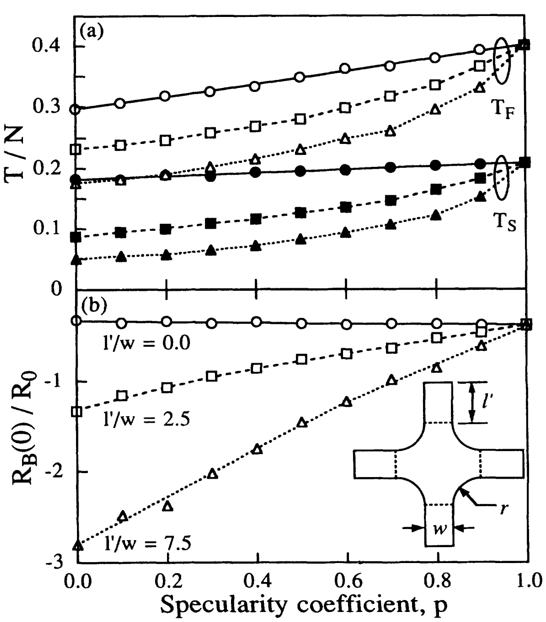

FIG. 2. Variation of T_F, T_S, and $R_B(0)$ with specularity coefficient p in a four-probe geometry with $r/w=2$ for three values of normalized lead length: $l'/w=0$ (solid lines), $l'/w=2.5$ (dashed lines), and $l'/w=7.5$ (dotted lines). (a) T_F (upper traces) and T_S (lower traces). (b) $R_B(0)$, and inset showing four-probe geometry.

equal probabilities of reaching any probe, thereby reducing $R_B(0)$. Also, the fact that $R_B(0)$ is still negative when $p=0$ indicates that $R_B(0)$ is dominated by trajectories that pass straight through the junction without suffering any boundary scattering.

In order to determine the effect the leads have in the presence of diffuse scattering, we looked at the angular distribution $P(\alpha)$ of the electrons entering the junction through a lead of length $l'/w=7.5$. At magnetic field $\beta=0$ [Fig. 3(a)] we see that for completely specular boundary scattering the injected distribution $[P(\alpha)=(\frac{1}{2})\cos\alpha]$ is preserved, independent of the lead length. For diffuse boundary scattering the distribution becomes more peaked in the forward direction, since electrons injected with large angles relative to the lead axis will suffer more boundary collisions within the lead and therefore be more likely to be backscattered before reaching the junction. Also, electrons scattered diffusely from large-angle trajectories to small-angle trajectories contribute to the increase in $P(\alpha)$ around $\alpha=0$. This "diffuse collimation" of the electron distribution will tend to increase the negative bend resistance, since those electrons that reach the junction will be more likely to go straight across, rather than be scattered into one of the side leads.

The enhancement of the quenching of R_H at $\beta\approx 0.1$ was also found to be a property of the leads rather than of the junction and so was also investigated in terms of the electron distribution injected into the junction from nonzero length leads. Figure 3(b) shows the angular distribution of electrons entering the junction through a lead of length $l'/w=7.5$ at a magnetic field $\beta=0.1$. As in the case of the enhancement of $R_B(0)$, the electron distribution becomes more peaked in the forward direction with the introduction of diffuse boundary scattering, but in this case the center of the distribution is shifted off center by the Lorentz force. The trajectories that will now dominate the Hall resistance are those that suffer a single boundary collision within the junction [Fig. 3(b), inset]. At the collision point within the junction, the "correct" lead (the lead towards which the electron is directed by the Lorentz force) is shadowed by the corner, so the electron is more likely to enter the "wrong" lead upon reflection, thus contributing to the negative R_H. Once again, the enhancement is effective even for completely diffuse boundary scattering.

We have also studied the effect of diffuse boundary scattering on the longitudinal resistance $R_L \equiv R_{14,23}$ of the six-probe device, and have compared the simulation results with low-temperature measurements taken on a 10-μm-long multiprobe wire fabricated in $GaAs/Al_xGa_{1-x}As$ heterostructure material (mobility, $\mu=4.5\times10^5$ $cm^2\,V^{-1}\,s^{-1}$; electron density, $N_s=3\times10^{11}$ cm^{-2}) using ion-implanted p-type gates to provide the lateral confinement.[11] The dashed line in Fig. 4 shows R_L as calculated for a device with $l/w=20$ and $r/w=2$, and 1.7-K measurements of R_L for the 10-μm-long wire are shown for comparison. A forward bias of 1.35 V is applied to the confining p-type gates, and under this condi-

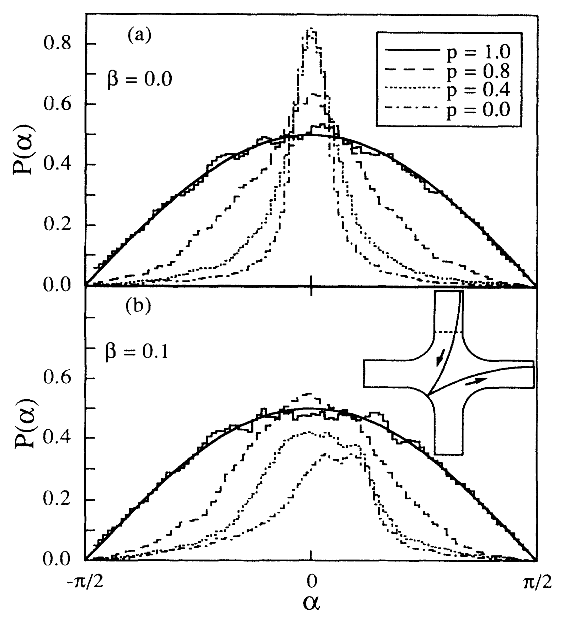

FIG. 3. Histograms of angular distribution at (a) $\beta=0.0$ and (b) $\beta=0.1$ of electrons entering the junction of a four-probe device from a lead of normalized length $l'/w=7.5$, for four values of the specularity coefficient p. Electrons are injected into the lead with a $(\frac{1}{2})\cos\alpha$ distribution (smooth solid lines). Inset: schematic device geometry showing the plane at which the angular distribution is taken (dashed line), as well as a representative trajectory for an electron entering the "wrong" lead, and so contributing to the quenching of R_H.

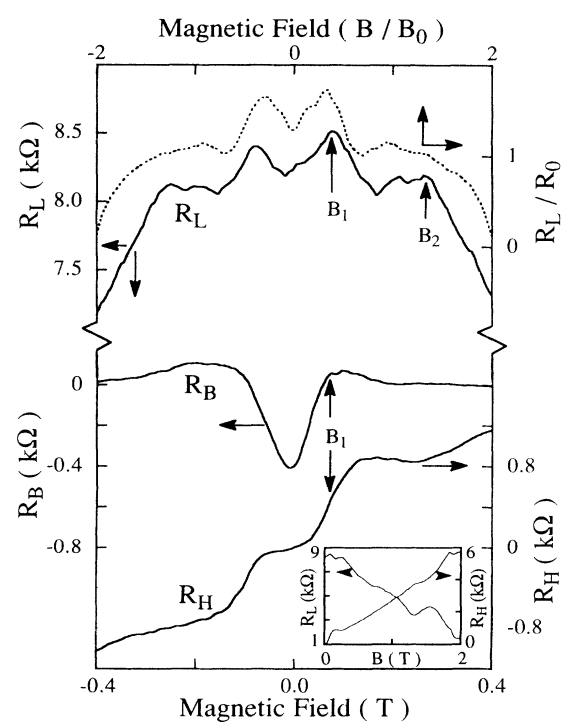

FIG. 4. Measured low-magnetic-field characteristics R_L, R_B, and R_H (solid lines) and calculated R_L (dashed line) in a multiprobe conductor. Inset: high-magnetic-field-measured R_L and R_H.

tion the electrical width of the wire is $W_e = 0.15 \pm 0.03$ μm, calculated from the position of the diffuse boundary scattering peak in the magnetoresistance.[12]

We find that when some diffuse scattering is included ($p = 0.8$) the model predicts two peaks in the longitudinal magnetoresistance (B_1 and B_2). The peak at B_1 is caused by scattering effects within the junctions[6] and has not previously been experimentally verified. The peak at B_2 is due to enhanced backscattering of the electrons by diffuse boundary scattering within the wire, and has previously been observed in wires fabricated using low-energy ion damage.[12] Both peaks are evident in our measurements, with approximately the correct relative field positions and relative magnitudes. Under the experimental conditions used there are a relatively large number of occupied subbands in the wire (~ 15), which is why the classical model predicts well the features in the magnetoresistance. However, contrary to the experimental results, the model predicts that R_L is zero for $\beta > 2$. This is because forms of random scattering other than diffuse boundary scattering are not included in the model.

Measurements of the Hall resistance R_H and the bend resistance R_B are also shown in Fig. 4. We see that a complete set of weak-magnetic-field resistance anomalies is present in both R_H (quenching around $B = 0$ and a last Hall plateau beginning at $B \approx B_l$) and R_B [negative $R_B(0)$ with a positive overshoot at $B \approx B_l$]. In the high-magnetic-field measurements (Fig. 4 inset) we observe quantum Hall plateaus in R_H and oscillations in R_L, indicating that the wire is of high quality. The assumption that electron transport across the wire and the junction is ballistic can be assumed to be valid, justifying our interpretation of the features observed at B_1 and B_2. A more detailed comparison between the simulation results and measurements on devices fabricated using ion implanted gates is presented elsewhere.[13]

In summary, we have shown how the previous discrepancy between the predicted and the measured magnitude of the negative zero-field bend resistance can be accounted for by incorporating diffuse boundary scattering into the semiclassical ballistic model. We also predict that the quenching of the Hall effect in a narrow junction is enhanced by diffuse boundary scattering. These effects are due to "diffuse collimation" of the electron distribution by diffuse boundary scattering within the leads attached to the junction. Diffuse boundary scattering also causes a second peak to appear in the longitudinal magnetoresistance; we have confirmed this experimentally with measurements on a wire fabricated in a $GaAs/Al_xGa_{1-x}As$ heterostructure material using ion-implanted p-type gates to provide the lateral confinement.

We thank the members of the Microelectronics Research Centre and the Hitachi Cambridge laboratory for useful discussions.

[1] For reviews, see *Nanostructure Physics and Fabrication,* edited by M. A. Reed and W. P. Kirk (Academic, New York, 1989), and C. W. J. Beenakeker and H. van Houten, in *Solid State Physics: Advances in Research and Applications,* edited by H. Ehrenreich and D. Turnbull (Academic, New York, 1991), Vol. 44, pp. 1–228.

[2] M. L. Roukes, A. Scherer, S. J. Allen, Jr., H. G. Craighead, R. M. Ruthen, E. D. Beebe, and J. P. Harbison, Phys. Rev. Lett. **59**, 3011 (1987).

[3] G. Timp, H. U. Baranger, P. de Vegvar, J. E. Cunningham, R. E. Howard, R. Behringer, and P. M. Mankiewich, Phys. Rev. Lett. **60**, 2081 (1988).

[4] Y. Takagaki, K. Gamo, S. Namba, S. Ishida, S. Takaoka, K. Murase, K. Ishibashi, and Y. Aoyagi, Solid State Commun. **68**, 1051 (1988).

[5] C. J. B. Ford, T. J. Thornton, R. Newbury, M. Pepper, H. Ahmed, D. C. Peacock, D. A. Ritchie, J. E. F. Frost, and G. A. C. Jones, Phys. Rev. B **38**, 8518 (1988).

[6] C. W. J. Beenakker and H. van Houten, Phys. Rev. Lett. **63**, 1857 (1989).

[7] C. W. J. Beenakker and H. van Houten, in *Electronic Properties of Multilayers and Low-Dimensional Semiconductor Structures,* edited by J. M. Chamberlain, L. Eaves, and J. C. Portal (Plenum, New York, 1990), pp. 75–94.

[8] H. U. Baranger, D. P. DiVincenzo, R. A. Jalabert, and A. D. Stone, Phys. Rev. B **44**, 10 637 (1991).

[9] M. Büttiker, Phys. Rev. Lett. **57**, 1761 (1986).

[10] M. L. Roukes and O. L. Alerhand, Phys. Rev. Lett. **65**, 1651 (1990); T. Sakamoto, Y. Takagaki, K. Gamo, S. Namba, S. Takaoka, and K. Murase, Solid State Commun. **80**, 535 (1991).

[11] R. J. Blaikie, K. Nakazato, B. Fraboni, D. G. Hasko, J. R. A. Cleaver, and H. Ahmed, Microelectronic Engineering **13**, 373 (1991).

[12] T. J. Thornton, M. L. Roukes, A. Scherer, and B. Van de Gaag, Phys. Rev. Lett. **63**, 2128 (1989).

[13] R. J. Blaikie, K. Nakazato, T. J. Thornton, J. R. A. Cleaver, and H. Ahmed (unpublished).